Supplementary methodology

Evaluation of robust normalizers suitable for qPCR analysis of mRNA levels in cardiac tissues from non-diabetic, STZ-diabetic and TETA-treated diabetic rats

Real-time qPCR is a powerful method for analysing changes in gene expression in tissues[1,2]. Data normalization using sufficiently robust normalizers is crucial for accurate quantification of mRNA expression[1-4]. In this experiment, we measured expression-stability of 12 candidate reference genes (CRGs) (*18S rRNA, Gapdh, Actb, B2m, Hprt1, Ubc, Ndc1, Ppia, Rpl13a, U2af, Tbp and Ywhaz*) to identify stably-expressed CRGs that are suitable for use as robust normalizers for qPCR analysis of mRNA levels in cardiac tissues from non-diabetic, diabetic and TETA-treated diabetic rats. The objective of selecting robust normalizers was to avoid errors that all too frequently occur with the use of single-gene normalizers. This approach is consistent with international best-practice recommendations for quantitative measurements of mRNAs by RT-qPCR[5].

RT-qPCR was performed using a LightCycler 480 System (Roche) according to the manufacturer's instructions, with SYBR Green I Master Mix (Roche). Reactions were performed in triplicate in 384-multiwell plates with pre-incubation for 5 min at 95°C, followed by 45 cycles, each of 10 s at 95°C, 15 s at 60°C and 20 s at 72°C. In each qPCR run, a standard curve for each respective gene was generated using the 6-point dilution series (which ranged between 0.01 and 25 ng). To check for possible genomic DNA contamination and multiplex products, a melting curve was generated for every run. The sequences of each gene-specific primer pair used are shown in Suppl. Table 2 below.

For data analysis, Threshold-values (crossing point Cp) and relative mRNA concentrations of each given reference gene were obtained for every qPCR reaction using LC 480 Software v1.5 (Roche). Stability of each reference genes was analyzed using the geNorm (GN)[6] and NormFinder (NF)[1,3] algorithmic approaches: **http://medgen.ugent.be/~jvdesomp/genorm/** and **http://www.mdl.dk/publicationsnormfinder.htm**, respectively. We found that *Rpl13a, Tbp* and *Ndc1* are most stably-expressed CRGs, and the geometric mean of the expression of these three CRGs forms a best robust normalizer for qPCR analysis in the selected cardiac tissues. This study has therefore used this robust normalizer to measure relative mRNA expression of genes involved in regulation of copper transport, as presented in Suppl. Table 2 below. *S*tatistical analysis was performed using unpaired Student's *t*-tests for pairwise comparisons and/or ANOVA for between-group comparisons. This statistical approach was deemed adequate as the comparisons made were *a priori* defined.

Supplementary References:

1. Andersen, C., Jensen, J. L., & Orntoft, T. Normalization of real-time quantitative reverse transcription-PCR data: a model-based variance estimation approach to identify genes suited for normalization, applied to bladder and colon cancer data sets. *Cancer Res* **64**, 5245-5250 (2004).
2. Van Guilder, H., Vrana, K. & Freeman, W. Twenty-five years of quantitative PCR for gene expression analysis. *BioTechniques* **44**, 619-629 (2008).
3. Jafari Anarkooli, I., Sankian, M., Ahmadpour, S., Varasteh, A. & Haghir, H. Evaluation of Bcl-2 family gene expression and caspase-3 activity in hippocampus of STZ-induced diabetic rats. *Exp Diabetes Res* **638467**, 1-6 (2008).
4. Mane, V., Heuer, M., Hillyer, P., Navarro, M. & Rabin, R. Systematic method for determining an ideal housekeeping gene for real-time PCR analysis. *J Biomol Tech* **19**, 342-347 (2008).
5. Bustin, S.A.*, et al.* The MIQE guidelines: minimum information for publication of quantitative real-time PCR experiments. **55**, 611-622 (2009).
6. Vandesompele, J.*, et al.* Accurate normalization of real-time quantitative RT-PCR data by geometric averaging of multiple internal control genes. *Genome Biol* **3**, R0034 (2002).

Supplementary Table 1. Sequences of primers used for qPCR analysis.

Gene name	Symbol	Sequences (5'-3')
COX17 cytochrome c oxidase copper chaperone	*Cox17*	tcaggagaagaagcctctgaa ttctcctttctcaatgatgcac
COX11 cytochrome c oxidase copper chaperone	*Cox11*	gtggtcccagagttctcacag; catgcatatacaggcaaaacg
SCO1 cytochrome c oxidase assembly protein	*Sco1*	ggatctttattggctggaatga; gtaaaggcttcccaatgctg
SCO2 cytochrome c oxidase assembly protein	*Sco2*	caacaacagcggacagagg; cagggcagtgagtaaaaccaa
Cytochrome c oxidase subunit I, mitochondrial	*Mt-CoI*	gctggaacaggatgaacagtat; tcctaagatagaagacaccccggcta
Cytochrome c oxidase subunit II, mitochondrial	*Mt-CoII*	caagcacaatagacgcccaagaa; agaattcgtagggagggaaggg
Cytochrome c oxidase subunit III, mitochondrial	*Mt-CoIII*	tttgaagccgcagcatgatact; ttttttttttttttttttttttttaggatc
Transcription factor A, mitochondrial	*tfam*	ctgatggccattacatgtgg aaagcccggaaggttcttag
Single stranded DNA binding protein 1	*ssbp1*	tggcttatcagtatgtgaaaaagg; atccatgtattcaccatagtccac
PPAR-gamma co-activator 1 alpha	*Pgc1α*	ggcacgcagtcctattcatt; tcctttggggtctttgagaa
18S ribosomal RNA	*18S*	aaatcagttatggttcctttggtc gctctagaattaccacagttatccaa
Beta-actin	*Actb*	gctgtattcccctccatcgtg cacggttggcctttagggttcag
Glyceraldehydes-3-phosphate dehydrogenase	*Gapdh*	tgacgtgccgcctggagaaa agtgtagcccaagatgccccttcag
Beta-2-microglobulin	*B2m*	ttctggtgccttgtctcactga cagtatgttcggcttcccattc
Hypoxanthine guanine phosphoribosyl transferase	*Hprt1*	gcttgctggtgaaaaggacctctcgaag ccctgaagtactcattatagtcaagggcat
Ubiquitin C	*Ubc*	aggtcaaacaggaagacagacgta tcacacccaagaacaagcaca
Peptidylprolyl isomerase A	*Ppia*	cgcgtctccttcgagctgtttg tgtaaagtcaccaccctggca
U2 auxiliary factor 36 kDa subunit	*U2af*	ccattgccctcttgaacatt

		cttccccgtacttctcttcc
Phospholipase A2	*Ywhaz*	tcttgtcaccaaccattcca aggggaagcgggtatcttag
Ribosomal protein L13a	*Rpl13a*	acaagaaaaagcggatggtg; ttccggtaatggatctttgc
TATA box binding protein	*Tbp*	agaacaatccagactagcagca; gggaacttcacatcacagctc
NDC1 transmembrane nucleoporin	*Ndc1*	ttcccaaagcatggattagc; cagccagacatggtagagca
Haemoglobin-alpha	*GloA*	caccaagacctacttccctcactt agagcatcggcgaccttct
Cytochrome b	*CytB*	ccacttcatcttaccatttattatcgc ttttatctgcatctgagtttaatcctgt

Supplementary full-length images of the western blot gels for Fig 1B and 1C, Fig 2B and 2C, Fig 3B, Fig 4E and 4F and 4G, Fig 7B.

Fig.1B

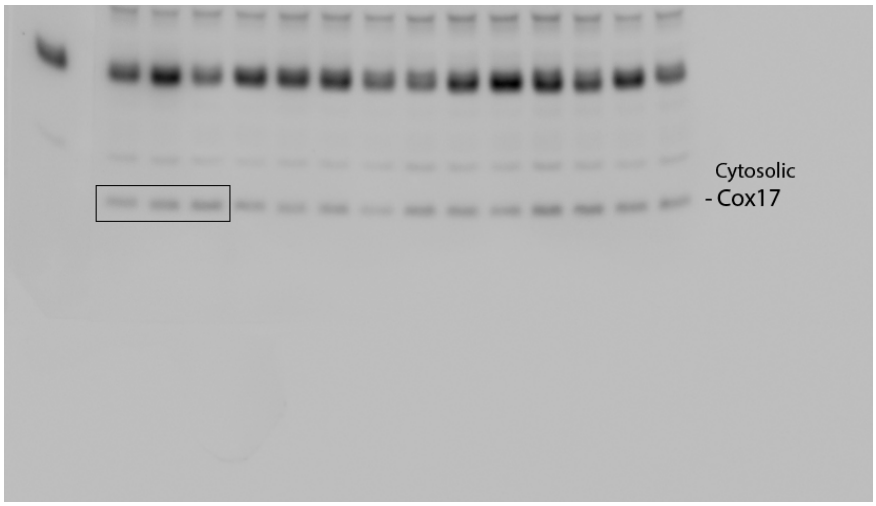

Full-length images of the western blot gels for Fig. 1B with approximate cropped regions used for figures marked with rectangles.

Fig. 1C

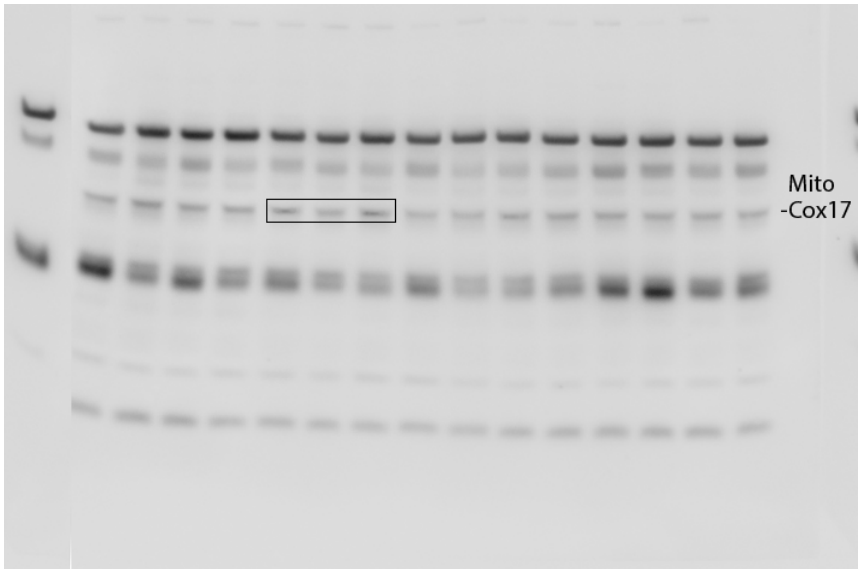

Full-length images of the western blot gels for Fig. 1C with approximate cropped regions used for figures marked with rectangles.

Fig. 2B

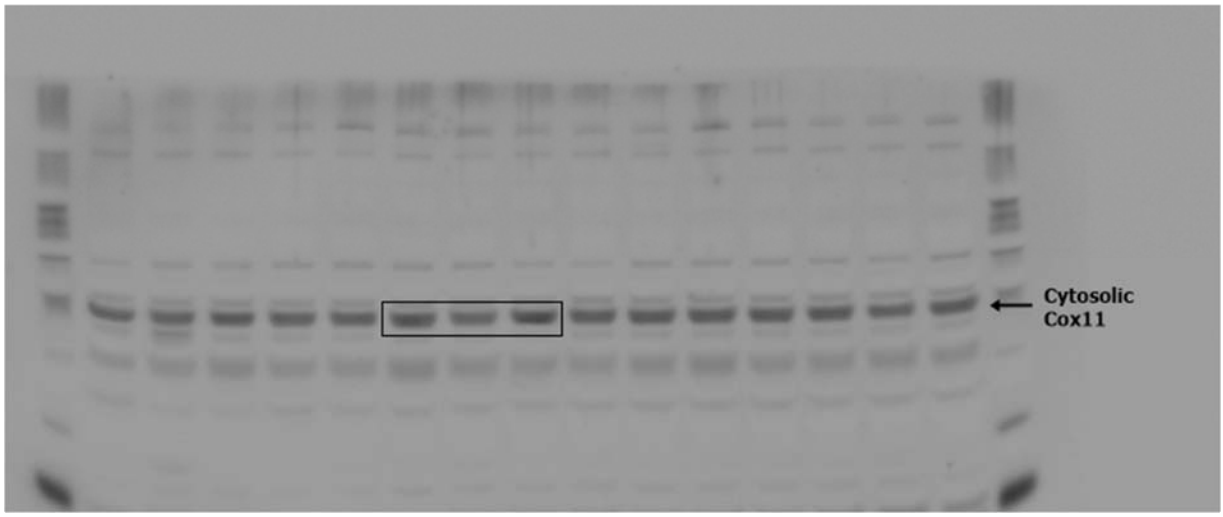

Full-length images of the western blot gels for Fig. 2B with approximate cropped regions used for figures marked with rectangles.

Fig. 2C

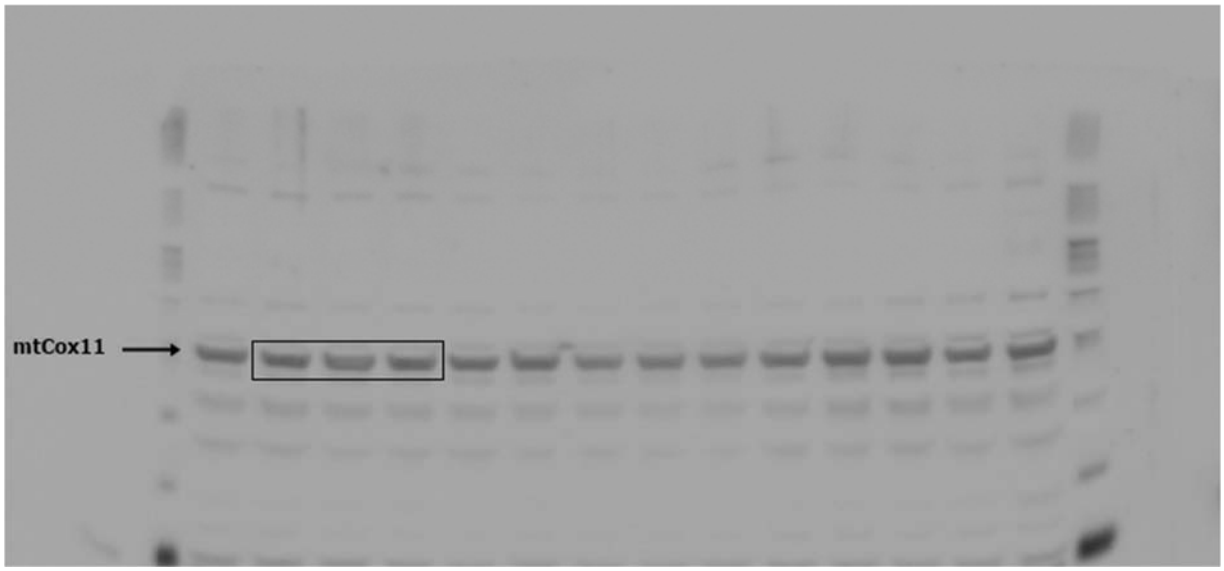

Full-length images of the western blot gels for Fig. 2C with approximate cropped regions used for figures marked with rectangles.

Fig. 3B

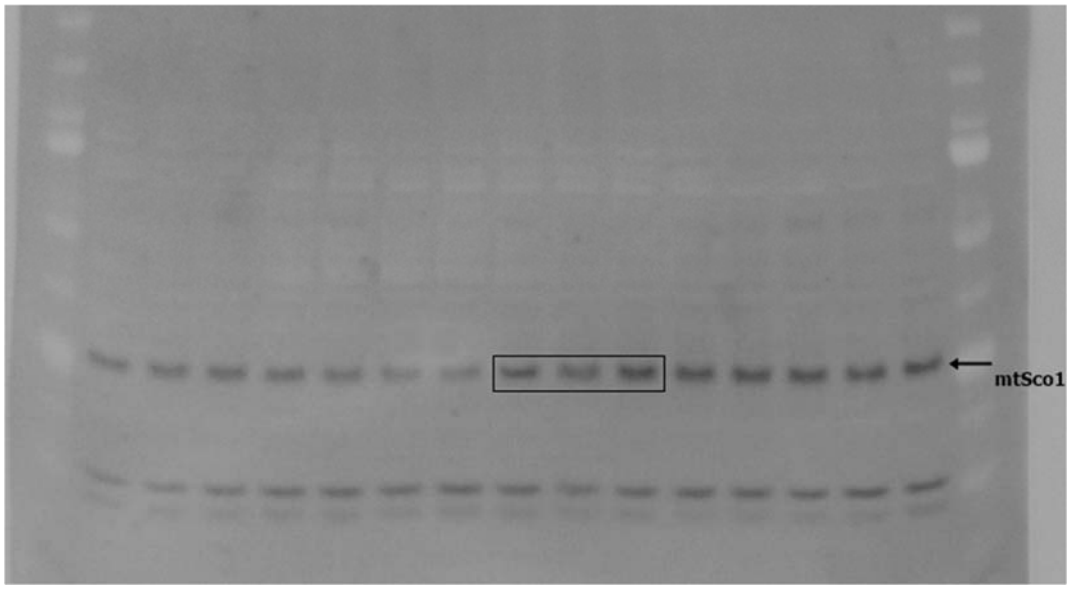

Full-length images of the western blot gels for Fig. 3B with approximate cropped regions used for figures marked with rectangles.

Fig. 4E

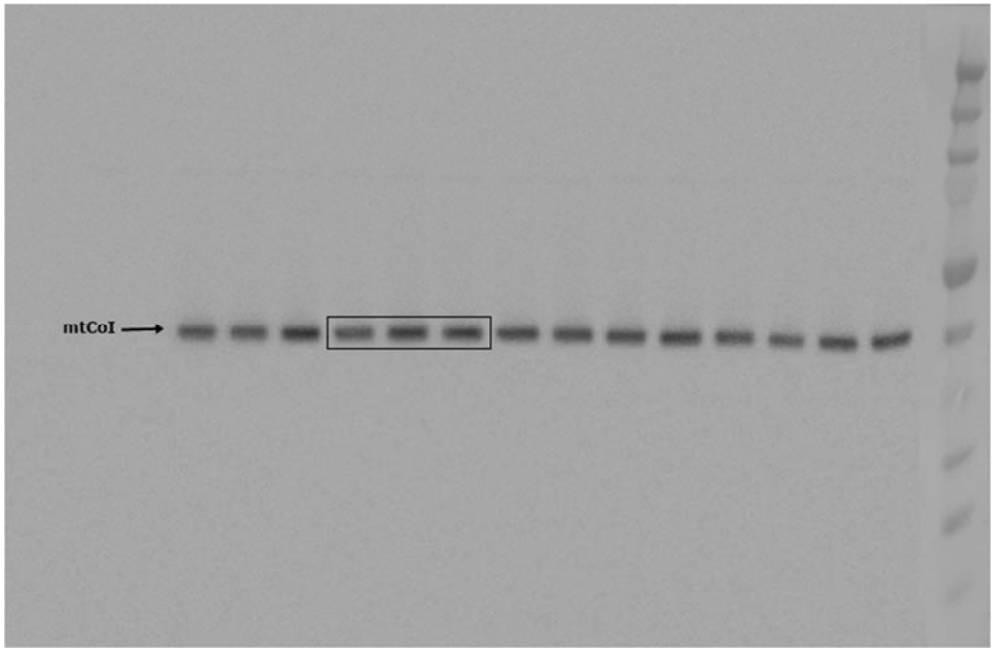

Full-length images of the western blot gels for Fig. 4E with approximate cropped regions used for figures marked with rectangles.

Fig. 4F

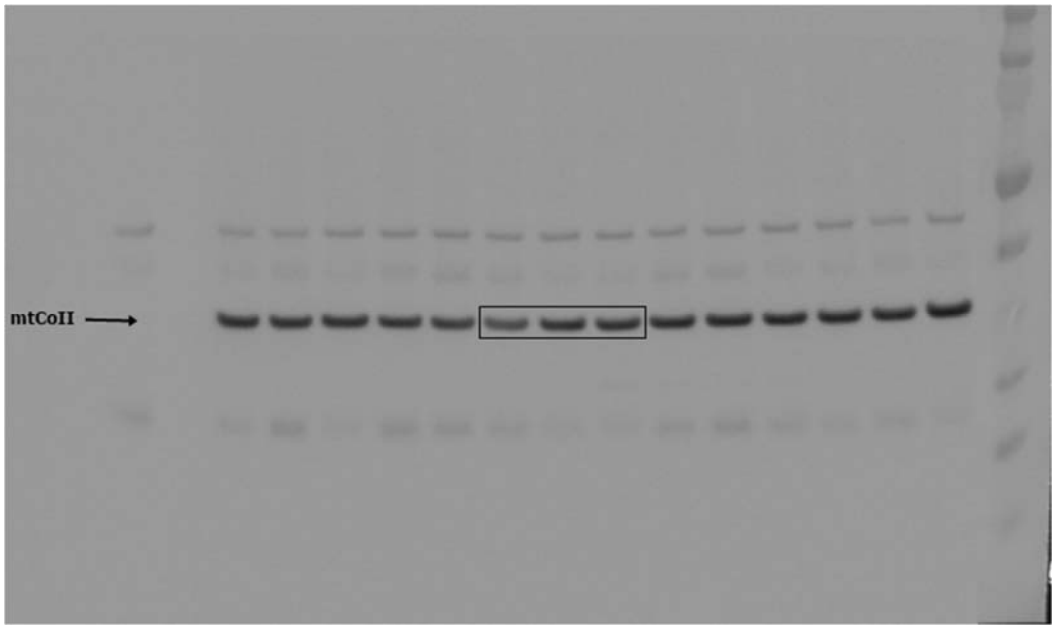

Full-length images of the western blot gels for Fig. 4F with approximate cropped regions used for figures marked with rectangles.

Fig. 4G

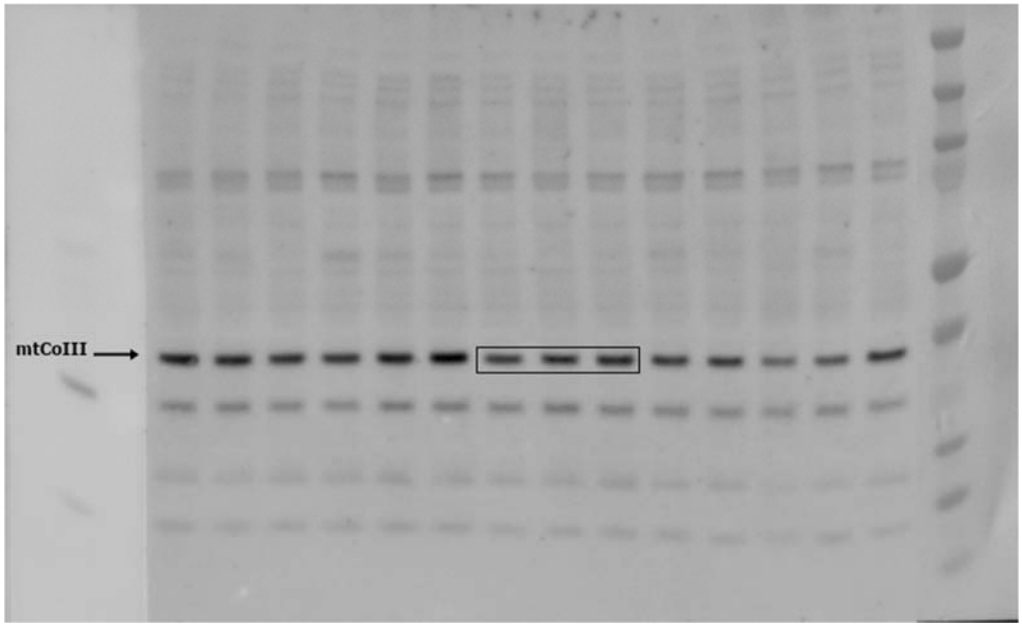

Full-length images of the western blot gels for Fig. 4G with approximate cropped regions used for figures marked with rectangles.

Fig. 7B

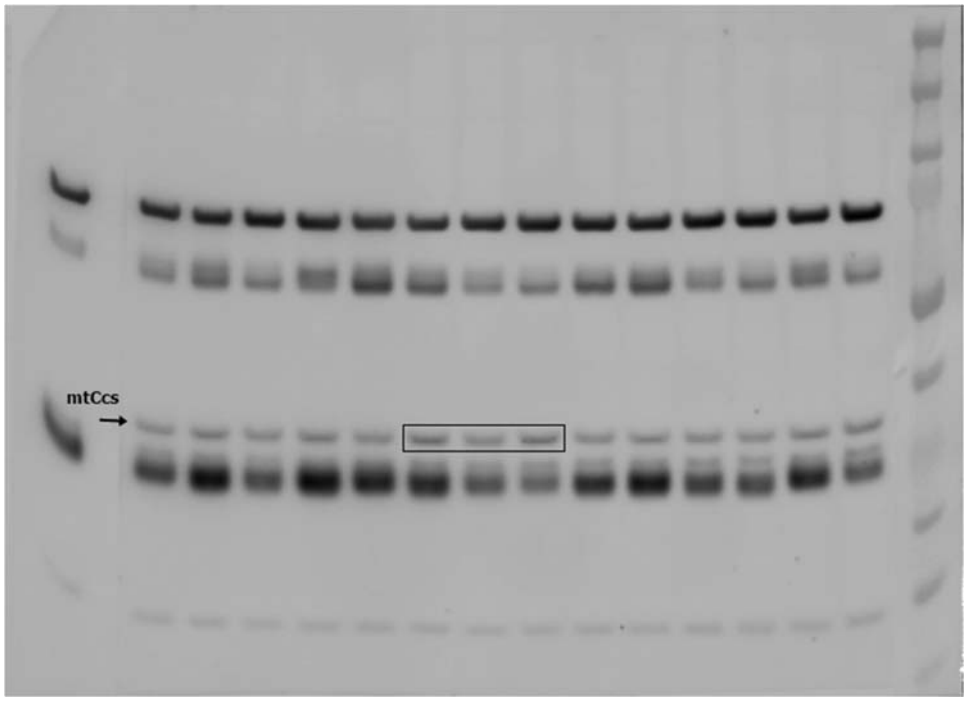

Full-length images of the western blot gels for Fig. 7B with approximate cropped regions used for figures marked with rectangles.

Supplementary Table 2. Relevant characteristics and hemodynamic parameters in isolated perfused hearts of normal control, diabetic, and TETA-treated diabetic male rats

Variable	Control	Diabetic	TETA-treated diabetic
Strain	Wistar	Wistar	Wistar
Age (weeks)	22-23	22-23	22-23
Body weight (g)	573 ± 16	220 ± 9*	290 ± 21*
Blood glucose (mM)	5.8 ±0.2	29.8 ± 0.7*	27.0 ± 1.2*
Heart weight (g)	1.58 ± 0.04	1.03 ± 0.06*	1.2 ± 0.1*
Heart weight/Body weight ($x10^{-3}$)	2.76 ± 0.01	4.7 ± 0.1*	4.1 ± 0.2*
Cardiac output (ml/min)	79.2 ±3.2	53.3 ± 8.1*	78.0 ± 4.0$^{\#}$
$+dP_{LV}/dt$ max (mmHg/s)	5840 ±1429	2249 ±162*	4082 ± 196$^{\#}$
$-dP_{LV}/dt$ min (mmHg/s)	-5795 ± 1472	-1952 ± 144*	-3366 ± 125$^{\#}$
Myocardial copper content (μg/g dry LV tissue)	50 ± 7	28.7 ± 2*	48 ± 6$^{\#}$

Measurements of steady-state cardiac function were made at 20 cm preload and 75 mmHg afterload of hearts paced at 300 beats/min. All values represent means ± SEM. Data were analysed using two-way ANOVA with post-hoc Tukey's tests. *$P < 0.05$ vs control; $^{\#}P < 0.05$ vs diabetic; n=9/group. Values of $-dP_{LV}/dt$ min demonstrate the occurrence of diastolic dysfunction in diabetic rats that was reversed by TETA-treatment, which also restored LV copper content to normal.

Supplementary images for Figure 1D.

Separate images for mt-CoII, DAPI, and WGA for the combined images shown in Fig. 1D.

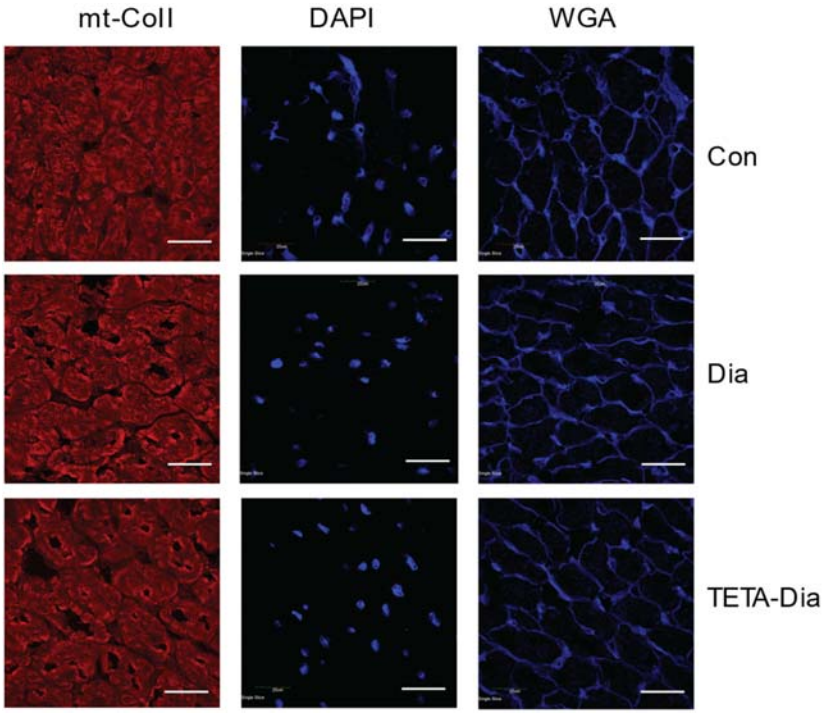

Supplementary images for Figure 2E.

Separate images for Cox11, DAPI, and WGA for the combined images shown in Fig. 2E

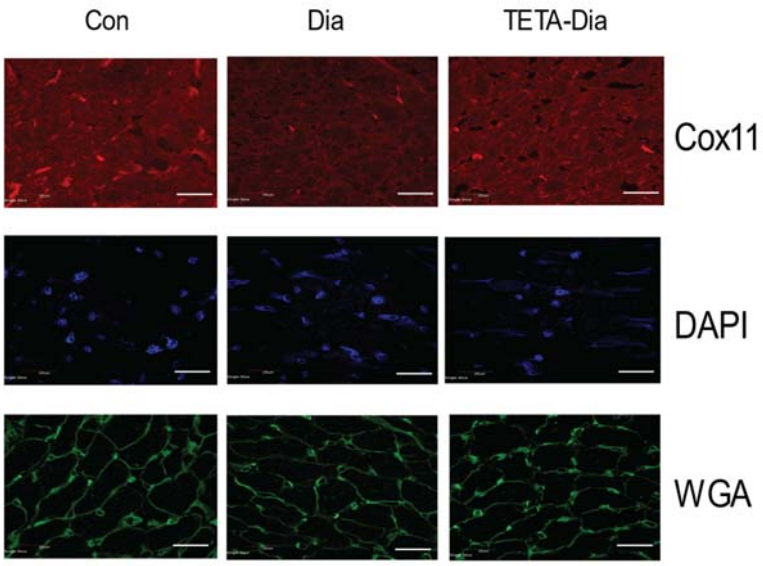

Supplementary images for Figure 3C.

Separate images for mt-CoII, DAPI, and WGA for the combined images shown in Fig. 3C.